Am J Physiol Gastrointest Liver Physiol 292: G913–G922, 2007.
First published November 30, 2006; doi:10.1152/ajpgi.00468.2006.

Intestinal ribosomal p70^{S6K} signaling is increased in piglet rotavirus enteritis

J. Marc Rhoads,[1,5] Benjamin A. Corl,[2] Robert Harrell,[2] Xiaomei Niu,[1] Lori Gatlin,[2] Oulayvanh Phillips,[2] Anthony Blikslager,[3] Adam Moeser,[3] Guoyao Wu,[4] and Jack Odle[2]

[1]*Department of Pediatrics, Ochsner Clinic Foundation and Ochsner Children's Research Institute, New Orleans, Louisiana;* [2]*Department of Animal Sciences and* [3]*College of Veterinary Medicine, North Carolina State University, Raleigh, North Carolina;* [4]*Faculty of Nutrition, Texas A&M University, College Station; and* [5]*Department of Pediatrics, University of Texas, Houston, Texas*

Submitted 10 October 2006; accepted in final form 23 November 2006

Rhoads JM, Corl BA, Harrell R, Niu X, Gatlin L, Phillips O, Blikslager A, Moeser A, Wu G, Odle J. Intestinal ribosomal p70^{S6K} signaling is increased in piglet rotavirus enteritis. *Am J Physiol Gastrointest Liver Physiol* 292: G913–G922, 2007. First published November 30, 2006; doi:10.1152/ajpgi.00468.2006.—Recent identification of the mammalian target of rapamycin (mTOR) pathway as an amino acid-sensing mechanism that regulates protein synthesis led us to investigate its role in rotavirus diarrhea. We hypothesized that malnutrition would reduce the jejunal protein synthetic rate and mTOR signaling via its target, ribosomal p70 S6 kinase (p70^{S6K}). Newborn piglets were artificially fed from birth and infected with porcine rotavirus on *day 5* of life. Study groups included infected (fully fed and 50% protein calorie malnourished) and noninfected fully fed controls. Initially, in "worst-case scenario studies," malnourished infected piglets were killed on *days 1*, *3*, *5*, and *11* postinoculation, and jejunal samples were compared with controls to determine the time course of injury and p70^{S6K} activation. Using a 2 × 2 factorial design, we subsequently determined if infection and/or malnutrition affected mTOR activation on *day 3*. Western blot analysis and immunohistochemistry were used to measure total and phosphorylated p70^{S6K}; [^{3}H]phenylalanine incorporation was used to measure protein synthesis; and lactase specific activity and villus-crypt dimensions were used to quantify injury. At the peak of diarrhea, the in vitro jejunal protein synthetic rate increased twofold (compared with the rate in the uninfected pig jejunum), concomitant with increased jejunal p70^{S6K} phosphorylation (4-fold) and an increased p70^{S6K} level (3-fold, $P < 0.05$). Malnutrition did not alter the magnitude of p70^{S6K} activation. Immunolocalization revealed that infection produced a major induction of cytoplasmic p70^{S6K} and nuclear phospho-p70^{S6K}, mainly in the crypt. A downregulation of semitendinosus muscle p70^{S6K} phosphorylation was seen at *days 1–3* postinoculation. In conclusion, intestinal activation of p70^{S6K} was not inhibited by malnutrition but was strongly activated during an active state of mucosal regeneration.

mammalian target of rapamycin; diarrhea; virus; malnutrition

ROTAVIRUS ENTERITIS causes 3.1 million episodes of diarrhea, 65,000 hospitalizations, and 125 deaths in the United States each year and costs ~$10 million annually (36). In pigs, after acute viral injury to the surface epithelium of the villi, rapid restoration of epithelial continuity depends on the migration of uninjured cells to cover denuded sections of the basement membrane. At the cellular level, enterocyte migration is a proliferation-independent process that generally is completed within 6–12 h and is followed by crypt cell proliferation to regenerate the villi. Previous studies from our laboratories and others have shown that migration requires nitric oxide (NO), prostaglandins, and polyamines (7, 17, 40–42, 57). Furthermore, migration was stimulated by the amino acid L-arginine by a process requiring protein synthesis and NO formation from L-arginine (42). Migration was impaired by amino acid deprivation and serum starvation, modeling a condition called protracted diarrhea of infancy in the malnourished host (19, 34).

Acute regulation of protein synthesis is achieved through changes in the rate of translation of mRNA via alterations in peptide chain initiation. A central mediator of this process is the mammalian target of rapamycin (mTOR). mTOR has been called a "nutrient sensor," capable of integrating amino acid and hormone levels with an organism's ability to survive (24, 48). mTOR activation results in the parallel phosphorylation and activation of two key mediators, p70 S6 kinase (p70^{S6K}; which phosphorylates ribosomal protein p70) and 4E-binding protein-1 (4E-BP1). Peterson et al. (39) reported that mTOR enhances p70^{S6K} phosphorylation indirectly by restraining a phosphatase. Phosphorylation of protein phosphatase 2A (PP2A) by mTOR in response to amino acids prevents the dephosphorylation of p70^{S6K}, placing p70^{S6K} in the activated state and activating the transcription of mRNAs with an oligopyrimidine tract that regulates ribosomal biogenesis (39).

mTOR is inhibited by individual and global amino acid starvation, and the macrolide rapamycin blocks p70^{S6K} reactivation by amino acids (54). The current experiments were designed to determine if during piglet rotavirus enteritis, the jejunal protein synthetic rate and jejunal mTOR signaling via p70^{S6K} would increase and if malnutrition would reduce the level of activation of p70^{S6K}.

METHODS

Materials

Rabbit anti-p70 S6 kinase antibody (A300-510) was purchased from Bethyl Laboratories (Montgomery, TX). Rabbit phospho-p70^{S6K} (Thr^{421}/Ser^{424}) antibody (no. 9204) and rabbit S6 ribosomal protein antibody (no. 2212) as well as rabbit phospho-S6 ribosomal protein (Ser$^{235/236}$) antibody (no. 2211) were from Cell Signaling Technology (Beverly, MA). Anti-actin antibody (A2066), protease inhibitor cocktail (P8340), and phosphatase inhibitor cocktails I (P2850) and II (P5726) were from Sigma (St. Louis, MO). Fluorophuor-conjugated donkey Alexa Fluor anti-rabbit IgG, anti-goat IgG (A-11057), 4′,6-diamidino-2-phenylindole (DAPI; D1360), and Prolong Gold Antifade Reagent (P36930) were all from Molecular Probes (Eugene, OR). Immunoblot polyvinylidene difluoride (PVDF) membranes were from

Address for reprint requests and other correspondence: J. M. Rhoads, Div. of Gastroenterology, Univ. of Texas Health Sciences Center, 6431 Fannin St., MSB 3.137, Houston, TX 77030 (e-mail: j.marc.rhoads@uth.tmc.edu).

The costs of publication of this article were defrayed in part by the payment of page charges. The article must therefore be hereby marked "*advertisement*" in accordance with 18 U.S.C. Section 1734 solely to indicate this fact.

Bio-Rad (catalog no. 162-0174, Hercules, CA). The Enhanced Chemiluminescence plus Western Blotting Detection System (ECL Plus) was purchased from Amersham Pharmacia Biotech (RPN2132, Piscataway, NJ). [^{3}H]phenylalanine was purchased from American Radiolabeled Chemicals (St. Louis, MO).

Animals and Experimental Design

All protocols were approved by the Institutional Animal Care and Use Committee of North Carolina State University. Pregnant sows were injected with 12.5 mg $PGF_{2\alpha}$ (Dinoprost, Pharmacia Upjohn, Kalamazoo, MI) on *day 112* of gestation to induce parturition. Piglets were collected directly from the birth canal, immediately cleaned with a 70% ethanol solution, and transported to a biosecure rearing facility. Piglets were housed individually within cages (length: 0.5 m; width: 0.3 m; and height: 0.4 m) contained in two rooms equipped with radiant heat sources to provide zonal temperatures of 32°C. Pigs were offered a milk diet via a gravity flow feeding system adapted from Oliver et al. (38). The composition of the full-strength formula exceeded piglet nutrient requirements (National Research Council, 1998) and was composed of commercial ingredients (Milk Specialties, Dundee, IL) as follows (in g/l): 93 dried skim milk, 45 Fatpack 80 (80% ether extract), and 12 vitamins/minerals. The dry matter content of the full-strength formula was 15% (vs. 7.5% for the malnourished groups; see below), and the calculated analysis (DM basis) was as follows: 31.1% crude protein, 36% lactose, 25% ether extract, and 4.6 Mcal/kg total energy. For the first 24 h, a liquid colostrum diet (LaBelle Associates, Bellingham, WA) was fed to provide passive immunity. Details of feeding rates were as reported by Zijlstra et al. (61). The fresh milk formula was offered 4 times/day (0800, 1300, 1800, and 2300 hour), and the milk reservoir and feeding apparatus for each pig were sanitized every 12 h. After 4 days of adaptation to the housing and feeding system, pigs were allocated to experimental treatments.

Extending our previously established malnutrition-rotavirus model (61, 62), in *experiment 1*, we used a total of 40 piglets distributed over 2 treatment regimens as follows: *1*) control noninfected animals fed full-strength formula or *2*) rotavirus-infected animals malnourished by feeding formula diluted 50% with electrolyte solution (1.91 g/l KCl, 0.15 g/l NaCl, and 1.65 g/l Na citrate). Intestinal samples were collected on *days 0*, *1*, *3*, *5*, and *11* postinfection.

In *experiment 2*, we further compared well-nourished and malnourished piglets ($n = 16$) that were allocated to a 2×2 factorial treatment scheme examining the effects of malnutrition and viral infection as follows: *1*) full-strength formula, noninfected (positive control); *2*) full-strength formula, rotavirus infected; *3*) malnourished (half-strength formula), noninfected; or *4*) malnourished, rotavirus infected (negative control). Based on the results from *experiment 1*, intestinal samples from *experiment 2* were collected only on *day 3* postinfection.

Rotavirus Inoculation and Clinical Measurements

The rotavirus inoculum, originally isolated by Lecce et al. (27), was passaged through colostrum-deprived sentinel pigs and prepared as a bacteria-free intestinal supernatant. Rotavirus ($\sim 10^7$ particles) and sham inoculants were suspended in 20 ml of full-strength milk formula, and piglets were gastrically intubated at 1000 hours on *day 4*. Previous investigations used 2×10^8 particles, but this dose resulted in a high mortality rate in preliminary experiments. Therefore, in a pilot experiment, we lowered the dose down to 10^7 particles, which gave consistent infections with negligible mortality.

Animal weights and feed intakes were measured daily. Feces were given a consistency score of *0*, *1*, *2*, or *3*, indicating firm, soft but formed, runny, or severe watery diarrhea, respectively. Pigs were rectally swabbed with a cotton-tipped applicator daily for the detection of rotavirus shedding using a commercial latex agglutination assay (Virogen Rotatest, Wampole Laboratories, Cranbury, NJ).

Intestinal Sampling

On designated sampling days, pigs were anesthetized with isoflurane and killed by American Veterinary Medical Association-approved electrocution followed by exsanguination. A heparinized blood sample was collected at this time, and plasma was stored at −20°C for amino acid analysis (59). Intestinal samples from the midjejunum area were collected, snap-frozen, and stored at −70°C until analysis by Western blotting. Intestinal segments were collected and fixed for histological analysis of intestinal morphology and immunohistochemical staining (38). Additional segments for in vitro measurements of protein synthesis were collected and used immediately. The mucosa was scraped, homogenized in PBS (pH 7.4), and stored at −20°C until assayed. The midjejunum was chosen because our previous studies identified this site as the region of maximal rotaviral injury in this model.

Analytical Procedures

Intestinal morphology and lactase specific activity were measured according to the procedures previously described (38).

Protein Synthesis

Protein synthesis was measured in vitro using intestinal explants prepared fresh from harvested tissue collected in *experiments 1* and *2*. Explants (totaling 50 mg) were incubated in 25-ml Erlenmeyer flasks with 3 ml medium 199 containing 0.5 μCi [^{3}H]phenylalanine for 2 h and maintained at 37°C in a shaking water bath. Following incubation, the tissue was removed from the flasks and immediately transferred to a tube containing 3 ml of 0.2 M perchloric acid. Explants were homogenized and centrifuged at 3,000 *g* for 20 min to separate proteins from free amino acids. The pellet was washed and centrifuged twice with 3 ml of 0.2 M perchloric acid and then incubated at 37°C for 90 min in 1.5 ml of 0.3 M sodium hydroxide to solubilize the protein pellet. Radioactivity was quantified by liquid scintillation counting, and protein synthesis calculated based on the specific activity of the radiolabeled phenylalanine in the media and the quantity found in the protein pellet.

Western Blot Analysis

The intestinal mucosa and muscle homogenates were prepared in RIPA buffer containing protease and phosphatase inhibitors. The protein concentration was determined using the Bio-Rad DC Protein Assay Kit (Bio-Bad) with BSA as the standard.

Determination of Phosphorylated p70^{S6K} and Total p70^{S6K}

Protein (40 μg) and an equal volume of 2× Laemmli sample buffer were combined; subsequently, samples were boiled for 5 min and electrophoretically separated by 7.5% SDS-PAGE. Protein was then transferred to a PVDF membrane with a semidry transfer cell. Membranes were incubated in blocking buffer (5% nonfat dry milk) in Tris-buffered saline (TBS; pH 7.6) plus 0.05% (vol/vol) Tween 20 (TBST) for 1 h at room temperature, followed by an incubation with p70^{S6K} phosphoralyted antibodies (1:3,000) in blocking buffer overnight at 4°C. After being washed with TBST, blots were incubated with the appropriate peroxidase-conjugated secondary antibody for 1 h at room temperature, and visualization of the protein was done with ECL Plus. The membrane was stripped for 30 min at 55°C. After being blocked for 1 h, total p70^{S6K} (1:3,000) and anti-actin were probed. Bands were detected with an enhanced chemiluminescence detection kit (ECL Plus, Amersham Biosciences). Quantitative data were obtained using a computer densitometer (Quantity One, Bio-Rad). Phosphorylated and total p70^{S6K} measurements were normalized to β-actin immunoreactivity.

Determination of Phosphorylated and Total Ribosomal Protein S6

We resolved proteins on a 15% acrylamide gel, followed by application of the appropriate primary antibody at 1:3,000 dilution, as described above. Results were normalized for β-actin immunoreactivity.

Immunohistochemistry

Tissues fixed in 4% formaldehyde were frozen sectioned (5-μm sections), and nonspecific binding was blocked by incubation of the slides with 5% normal donkey serum in 1% BSA in PBS for 15 min at room temperature. After being washed with PBS, slides were incubated for 90 min in 1% BSA in PBS containing primary antibodies at a 1:200 dilution. Slides were washed three times for 5 min each with PBS and then labeled with 1:500 dilutions of combined conjugated Alexa Fluor 488 donkey anti-rabbit IgG for 30 min at room temperature with light shielding. Slides were then stained with DAPI at 1:5,000 dilution in PBS for 2 min and subsequently mounted with Prolong Gold Antifade Reagent. Fluorescent images were captured with a Zeiss deconvoluting microscope at ×10 magnification with a ×60 immersion objective and with the use of Slidebook from Intelligent Imaging Innovations software (www.intelligent-imaging.com).

Statistical Analysis

Statistical comparisons were performed using ANOVA and *t*-tests for unpaired data (two-tailed) analysis (Statview4, Abacus Concepts, Berkely, CA) and using NCSS (www.ncss.com) for Wilcoxon signed-rank tests for paired analyses. Results are expressed as means ± SE, and $P \leq 0.05$ was considered statistically significant.

RESULTS

Effect of Rotavirus Infection on mTOR/p70S6K in Malnourished Piglets: Experiment 1

The initial studies were designed to determine the effects of rotavirus enteritis on gut protein synthesis and mTOR activation in a worst-case scenario, when malnourished piglets were infected with live rotavirus particles in the first week of life. Zijlstra et al. (61) previously showed that this design produces a more prolonged and severe illness in piglets, lasting 16 days. Thus, malnourished subjects were pair fed 50% of the per kilogram diet of their fully fed counterparts by formula dilution with electrolyte solution (see METHODS). Forty piglets, in groups of eight piglets across five time points, pair-matched infected-malnourished and noninfected pigs, were studied at each time point.

Jejunal in vitro protein synthesis. Over a 2-h assay period, we compared the in vitro protein synthetic rate. We found that the infected jejunum had a significant increase in the protein synthesis rate, ranging from 50% to 200% higher than that in the jejunum from uninfected pigs (Fig. 1). Furthermore, despite the malnutrition, there was a steady increase in the infected jejunal protein synthetic rate, which peaked at *day 5* postinoculation.

Jejunal levels of phosphorylated and total p70S6K. Immunoblots for p70S6K showed a band at a molecular mass of ~68 kDa (Fig. 2*A*). There was considerable variability in the total p70S6K level with postnatal age in uninfected pigs (with more immunoreactivity at *day 5* than earlier or later in the blot shown, reflecting the first litter of piglets). However, when averaged out with *day 1* uninfected pig jejunal p70S6K normalized to a densitometric value of 1.0, there was a small but statistically insignificant decrease in signal up to *day 11* in the

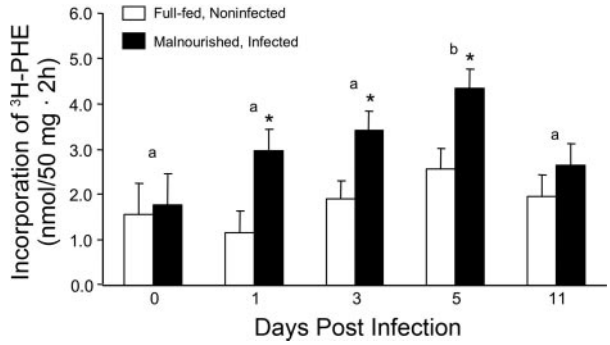

Fig. 1. In vitro protein synthesis of small intestine explants from fully fed, noninfected piglets and malnourished, rotavirus-infected piglets (*experiment 1*). [a,b]Different superscripts indicate a significant effect of time on protein synthesis, peaking at *day* (d)*5* ($P \leq 0.05$); *significant difference between malnourished, infected piglets and fully fed, noninfected controls when they were compared at a specific time point ($P \leq 0.05$).

noninfected pig jejunum. The most marked changes were increases in the jejunal levels of p70S6K and phosphorylated p70S6K at the peak of infection (*days 3* and *5*). Significant increases in p70S6K levels were seen on *days 3* and *5* postinoculation (2- and 2.5-fold increases in level). These results were confirmed in duplicate and were also confirmed by immunohistochemistry (see below).

We additionally found a strong induction of phosphorylated p70S6K in infected pigs at *day 3* and/or *day 5* postinoculation in each group of infected piglets (Fig. 2*A*). There was no observable phosphorylated p70S6K in uninfected jejunal samples at the same time points. Using a *day 1* control pig ratio of phospho-p70S6K to actin as "1.0," we normalized the densitometry data (shown in Fig. 2*B*). In summary, our data show that p70S6K was more abundant and more phosphorylated (activated), indicating mTOR activation during rotavirus infection.

Immunolocalization of p70S6K and phospho-p70S6K in normal and rotavirus-infected piglet jejunum. Viral enteritis has markedly different effects along the villus-crypt axis. For example, in piglets, villus tip cells are infected by the virus, whereas crypt cells undergo mitogenesis to regenerate the damaged villus tips (13, 22). Previous investigations of mTOR activation in the intestine used Western blot techniques (14). We are unaware of studies determining the histological site of local activation of mTOR in the diseased intestine. Using polyclonal antibodies to rat p70S6K, we found that the normal uninfected villus epithelium had very little immunoreactivity, whereas some immunoreactivity was found in the crypt epithelium and lamina propria of the villus core (subepithelial portion of the villus; Fig. 3*A*). We also found strong crypt cell immunoreactivity of the infected jejunal epithelium, and there was a highly significant increase in immunoreactivity of the infected tissue compared with control tissue (Fig. 3*A*). With respect to phospho-p70S6K, only scattered sites of crypt and villus core immunoreactivity were seen in uninfected jejunal tissues (Fig. 3*B*), whereas very strong staining was seen throughout the crypt epithelium and in small "patches" along the sides of some of the regenerating villi in infected tissues.

High-power microscopic analysis (Fig. 3*C*) showed that there was diffuse total p70S6K staining in enterocytes in the apical cytoplasm and basolateral cytosol. However, immuno-

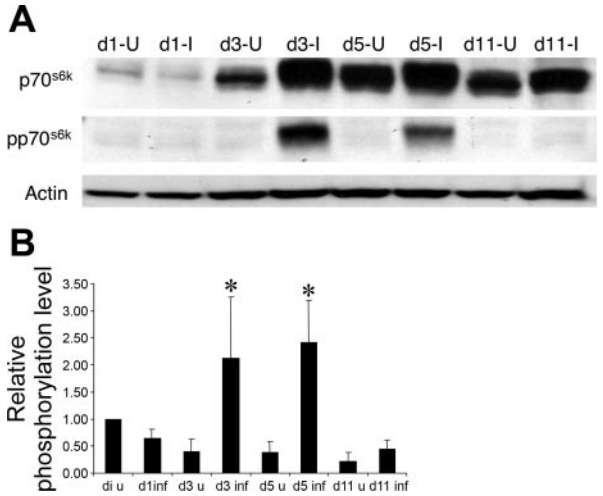

Fig. 2. *A*: effect of infection on jejunal p70 S6 kinase ($p70^{S6K}$) levels and phosphorylation. U, uninfected group; I, infected group; $pp70^{S6K}$, phospho-Thr^{421}/Ser^{424} $p70^{S6K}$. On *day 1* postinoculation, uninfected tissue had a low level of $p70^{S6K}$, which increased to a maximum on *day 5* postinoculation in this litter of pigs. However, in another litter, there was no trend toward an increase in $p70^{S6K}$ levels with age in uninfected animals. On *days 3*, *5*, and *11* postinoculation, there was a prominent increase in total $p70^{S6K}$. Furthermore, there was significant phosphorylation of $p70^{S6K}$ on *days 3* and *5* postinoculation. Actin levels were equivalent for each of the samples, indicating equal loading of the lanes. The results shown are representative of 2 paired groups of piglets. *B*: effect of rotavirus infection on intestinal $p70^{S6K}$ levels. Densitometric signals for $p70^{S6K}$ were normalized for the level of actin and expressed as multiples of 1.0. On *day 1*, the uninfected piglet jejunum was assigned a value of 1.0. The results shown are of $n = 3$ values at each time point. $^*P < 0.05$ compared with the infected group at the same time point and with *day 1* uninfected pigs.

reactivity of phospho-Thr^{421}/Ser^{424} $p70^{S6K}$ was predominantly in the nucleus (Fig. 3*C*, *right*).

Diarrhea and fecal rotavirus scores. We examined our clinical data to determine if the time of peak activation of mTOR coincided with the peak of the clinical illness. Compared with uninoculated piglets, which had soft stools (fecal scores of <1) throughout the study (Table 1), rotavirus-inoculated animals had diarrhea scores of 2–3, lasting from *days 2* to *9* after inoculation, indicating loose-watery diarrhea. Diarrhea scores peaked on *days 3* and *5* postinoculation, which corresponded to the peak activation of $p70^{S6K}$ by phosphorylation. Similarly, fecal rotavirus antigen scores peaked at *days 3–5* postinoculation.

Body weight and energy intake. We monitored clinical features daily to determine if gut protein synthesis and mTOR activation correlated with food intake. When fully fed, noninfected piglets thrived, gaining ~1.5 kg over the 11-day study period, or an increase of >75% in body weight, without any change in $p70^{S6K}$ phosphorylation. The malnourished-infected group had a plateau in body weight after inoculation and dietary restriction (Table 1). Although none of the rotavirus-infected pigs died, the oral energy intake was reduced to ~35% of normal in infected dilute milk-fed piglets (data not shown) for 1–2 days. Despite the reduced protein and calorie intake, the intestinal mTOR activation described above occurred in these malnourished piglets.

Jejunal mucosal histological features and lactase activity. Although the studies above confirmed peak clinical symptoms at the time of protein synthesis activation in the infected gut, it was important to verify that peak intestinal epithelial damage occurred during the same interval. Histological examination of jejunal tissues showed the most severe villus blunting and altered villus-to-crypt ratio at *days 3–5* (Table 2). Previously, our studies identified lactase as the most prominent disaccharidase marker of jejunal rotavirus infection, especially in the midjejunum (44). In the infected piglet jejunum, the current study showed a >50% decrease in jejunal lactase activity ($P < 0.05$; Table 2), with maximal blunting at *day 5*. Notably, these abnormalities persisted during the entire study period.

In summary, peak activation of jejunal protein synthesis and $p70^{S6K}$ phosphorylation corresponded to the peak of diarrhea and intestinal damage, at *days 3–5* postinoculation. Although diarrhea had improved and piglets began to gain weight, mucosal abnormalities persisted at *day 11*, beyond the period of maximal activation of $p70^{S6K}$.

Effect of Malnutrition Versus Full Feeding on Rotavirus Activation of mTOR: Experiment 2

Clinical response to infection. To separate the effects of malnutrition and infection on mTOR pathway activation during viral enteritis, we studied a separate group of piglets in a 2 × 2 factorial analysis. Control pigs fed full-strength formula with and without rotavirus infection were compared with 50% pair-fed malnourished piglets with and without rotavirus infection. Pigs were sampled on *day 3* postinfection based on the results of *experiment 1*. Infected animals weighed significantly less than uninfected controls (Table 3). Diarrhea scores, rotavirus scores, and the percentage body weight reduction during infection were not significantly different when well-nourished infected and malnourished-infected subjects were compared (Table 3). Infected piglets on the control diet (see below) had a reduction to 50% of normal intake on the day of infection, which returned to normal values on *day 6*.

Rotavirus infection produced an increase in the jejunal protein synthesis rate (incorporation of [^{3}H]phenylalanine) in vitro, with no difference in this response with respect to feeding regimen (Fig. 4*A*). When we compared intestinal mTOR activation in well-nourished pigs and their malnourished counterparts, we found a similar induction of $p70^{S6K}$ and phospho-$p70^{S6K}$ in all infected pigs regardless of whether they were malnourished (Fig. 4*B*). We conclude that rotavirus infection has a dominant effect on jejunal mTOR activation regardless of the state of nutrition.

Downstream signaling to ribosomal protein S6 in the intestine and skeletal muscle during infection. We obtained jejunal and semitendinosus muscle samples from uninfected and infected piglets at the same time points as those shown in Fig. 2. An antibody to phosphorylated and total ribosomal protein S6 was used to target $p70^{S6K}$ signaling during the course of infection. Figure 5, *top*, shows that in the intestine, the induction of mTOR signaling via $p70^{S6K}$ resulted in a major increase in the phosphorylation of ribosomal protein S6 ($n = 3$ observations, with similar findings in each pair of uninfected and infected subjects). Maximal induction occurred at *day 5* with a 3.5-fold increase in phosphorylation ($P = 0.054$ by the Wilcoxon signed-ranks test, $n = 3$).

Previously, investigators have shown that cardiac muscle protein synthesis decreases during the catabolic state induced in rats by lactose-induced diarrhea (44). From our animals,

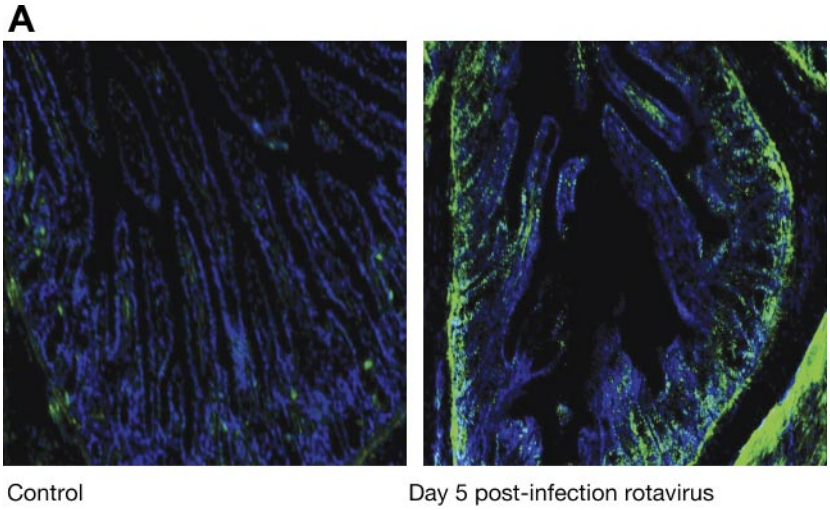

Fig. 3. *A*: immunohistochemical appearance of p70[S6K] in the jejunal mucosa of uninfected piglets (*left*) and *day 5* rotavirus-infected piglets (*right*). Note the intense (FITC; green) staining in the crypt region (and muscularis) of infected tissue only. Nuclei were stained with 4′,6-diamidino-2-phenylindole (blue). The results shown are representative of 3 observations at ×10 magnification. *B*: immunohistochemical appearance of pp70[S6K] in the jejunal mucosa of uninfected piglets (*left*) and *day 5* rotavirus-infected piglets (*right*). Note the intense (FITC; green) staining in the crypt region (and muscularis) of infected tissue only. Magnification: ×10. *C*: immunohistochemical appearance of p70[S6K] in the jejunal mucosa of *day 5* rotavirus-infected piglets (*left*) and pp70[S6K] in *day 5* rotavirus-infected piglets (*right*). In the *left*, note the diffuse (FITC; green) p70[S6K] staining in enterocytes in the apical cytoplasm (arrow) and basolateral cytoplasm (arrowhead); also, in the *right*, note the nuclear staining (FITC; green) of pp70[S6K] (arrow). Magnification: ×63.

semitendinosus muscle samples were subjected to immunoblot analysis to test the hypothesis that skeletal muscle mTOR signaling is reduced in rotavirus infection. Figure 5, *bottom*, shows that ribosomal protein S6 was strongly phosphorylated in muscle from the younger piglets at *days 1* and *3* and then tapered off in uninfected piglets. At these same time points, phosphorylation was markedly reduced (40–60% by densitometric analysis) in infected piglets ($P = 0.054$ at *days 1* and *3* postinoculation, $n = 3$). We additionally noted that the total S6 level declined with aging in uninfected 1- to 2-wk-old piglets.

Table 1. *Daily clinical measurements of piglets fully fed and noninfected or malnourished and infected with rotavirus (experiment 1)*

	Days Postinfection				
	Day 0	*Day 1*	*Day 3*	*Day 5*	*Day 11*
Diarrhea score					
Fully fed, noninfected	0.7	0.5	0.5	0.6	0.8
Malnourished, infected	1.1*	1.2*	2.0*	2.2*	1.5*
SE	0.1	0.1	0.1	0.2	0.3
Rotavirus shedding					
Fully fed, noninfected	0.0	0.0	0.0	0.0	0.0
Malnourished, infected	0.0	0.1	2.6*	3.0*	1.8*
SE		0.1	0.1	0.2	0.4
Body weight, kg					
Fully fed, noninfected	1.88	1.89	2.00	2.21	3.33
Malnourished, infected	1.91	1.83	1.73*	1.60*	2.05*
SE	0.03	0.02	0.04	0.06	0.07

*Significant effect ($P < 0.05$) of malnutrition and infection compared with fully fed and noninfected control piglets on the same day.

These findings suggested differential regulation of the mTOR pathway in the intestine (upregulation) and muscle (downregulation) during viral enteritis.

Serum amino acid levels. We initially hypothesized that serum levels of branched-chain and other amino acids might be reduced in malnourished-infected animals and that the reduced circulating levels might correspond to the reduced level of activation in the infected bowel. When we found activation of the mTOR pathway by viral enteritis, we predicted that serum levels would not be significantly reduced in the malnourished-infected group. In infected-malnourished piglets, serum levels of certain amino acids were significantly increased. This finding pertained to five amino acids (serine, phenylalanine, glutamin, tryptophan, and alanine); only citrulline was decreased

Table 2. *Small intestine lactase activity and intestinal morphology measurements of piglets fully fed and noninfected or malnourished and infected with rotavirus (experiment 1)*

	Days Postinfection				
	Day 0	*Day 1*	*Day 3*	*Day 5*	*Day 11*
Lactase activity, μmol·min^{-1}·g protein^{-1}					
Fully fed, noninfected	114.8†	109.7‡	85.9‡	101.0‡	88.9‡
Malnourished, infected	134.1	48.7*	42.7*	26.5*	29.1*
SE	21.4	14.8	13.3	13.3	14.8
Villus height, mm					
Fully fed, noninfected	1.00†	0.83‡	0.72§	0.60§	0.68§
Malnourished, infected	1.01	0.54	0.31*	0.30*	0.40*
SE	0.11	0.08	0.06	0.07	0.08
Crypt depth, mm					
Fully fed, noninfected	0.11	0.11	0.14	0.13	0.13
Malnourished, infected	0.12	0.11	0.12	0.13	0.12
SE	0.01	0.01	0.01	0.01	0.01
Villus height-to-crypt depth ratio					
Fully fed, noninfected	9.70†	7.69‡	5.85§	4.94§	5.32§
Malnourished, infected	8.18	4.83	2.73*	2.40*	3.42
SE	1.13	0.78	0.70	0.70	0.78

*Significant effect ($P < 0.05$) of malnutrition and infection compared with fully fed and noninfected control piglets on the same day; † ‡ §signficant effect ($P < 0.05$) of day across both treatments.

Table 3. *Clinical measurements of piglets fully fed or malnourished and infected or noninfected with rotavirus on day 3 postinfection (experiment 2)*

	Fully Fed		Malnourished			
	Noninfected	Infected	Noninfected	Infected	SE	Effect
Body weight, kg	2.13	1.93	1.95	1.72	0.1	F, V
Rotavirus shedding	0.0	3.5	0.0	3.4	0.2	V
Diarrhea score	0.3	2.8	1.3	3.0	0.5	V

V, significant main effect ($P < 0.05$) of rotavirus infection; F, significant main effect ($P < 0.05$) of feeding level. The interaction of V × F was not significant ($P > 0.05$).

(Table 4). The total amino acid concentration increased only 29% in infected-malnourished pigs. We conclude that the increased activation of mTOR/p70^{S6K} in the infected bowel was unlikely to be due to this minor change in the total circulating amino acid level.

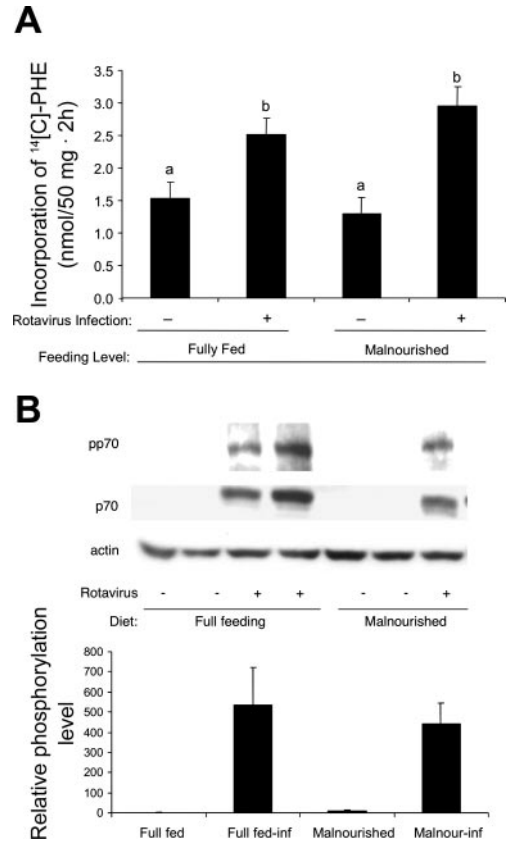

Fig. 4. *A*: in vitro protein synthesis of small intestine explants from piglets fully fed or malnourished (Malnour) and infected (Inf) or noninfected with rotavirus on *day 3* postinfection (*experiment 2*). ^{14}[C]-PHE, [^{14}C]phenylalanine. [a,b]Different superscripts indicate a significant difference. Protein synthesis rates increased in the jejunum of rotavirus-infected piglets ($P < 0.05$). The interaction between feeding level and infection was not significant ($P > 0.05$). *B*: impact of nutrition on gut p70^{S6K} phosphorylation during infection. The results shown are representative blots of total p70^{S6K}, pp70^{S6K}, and actin. The level of pp70^{S6K} (*top*) increased in infected piglets in both the well-nourished group and malnourished group. Note that the total level of p70^{S6K} was increased in fully fed (*middle left*) and malnourished (*middle right*) piglets; n = 3–4 piglets were studied at each time point, and the results were combined. Normalized densitometric values for pp70^{S6K}/total p70^{S6K} (divided by actin) are shown in the bar graph (*bottom*). The induction of p70^{S6K} was equivalent in fully fed and malnourished piglet jejunum.

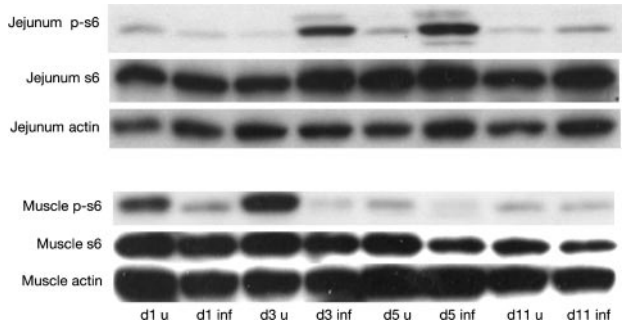

Fig. 5. Effect of rotavirus on intestinal and muscle levels of phospho-ribosomal protein S6 (p-S6) and total ribosomal protein S6. Jejunal samples were excised from uninfected and infected animals on *days 1*, *3*, *5*, and *11* postinfection. *Top*: infected piglet jejunum showed markedly increased p-S6 and total S6 protein on *days 3* and *5* postinfection. *Bottom*: both uninfected and infected semitendinosus muscle tissues showed a reduction of total S6 protein from *day 1* to *day 11*. However, rotavirus infection produced a major reduction (~50%) in p-S6 in muscle on *days 1* and *3* postinoculation compared with uninfected controls ($P = 0.054$ on *days 1* and *3* postinoculation.) Results are representative of 3 replications.

DISCUSSION

Intestinal Protein Synthesis Is Activated During Rotavirus Enteritis

Previous investigations of rotavirus enteritis have shown virus invasion and apoptosis at the tips of infected villi (9, 28). In the piglet model, we (44) have shown that the site of maximal injury is the midjejunum. At this site, rapid crypt cell proliferation characterized by increased thymidine kinase activity and crypt cell mitosis has been demonstrated (13). During this reparative phase of rotavirus infection, we are unaware of previous investigations of protein synthesis in the intestine. However, diarrheal disease has been shown to coexist with reduced protein synthesis in other organs, such as the heart (20). Our investigation showed a 50–100% increase in radioactive phenylalanine incorporation into intestinal protein at *days 1*, *3*, and *5* postinoculation. By *days 3–5* postinoculation, when the diarrhea was relatively severe, villus-to-crypt ratios were markedly altered to ~2.5, or ~50% of the normal ratio. Corresponding to the increase in protein synthesis was an increase in cell proliferation and expansion of the crypt. Our previous study (44) showed a sevenfold elevation in the intestinal level of thymidine kinase during the first 8 days of rotavirus inoculation, which decreased after this time point. Even in uninfected piglets, there was a less severe (50%) reduction in villus-to-crypt ratio during early postnatal life in uninfected piglets. Control piglets were highly unlikely to have had intestinal infection because they were without diarrhea and were raised artificially in our barrier-intact facility (43). Also supporting the concept that rotavirus infection led to a "proliferative" epithelium, villi of the infected piglet jejunum were populated by less-differentiated enterocytes, as demonstrated by the severe reduction in lactase specific activity (<10% of normal).

Intestinal p70^{S6K} Is Activated During Rotavirus Enteritis

In this infected epithelium, there was a marked (>3-fold) increase in both p70^{S6K} level and mTOR activation as determined by both the phosphorylation of p70^{S6K} and of its downstream target ribosomal protein S6. The activation was most evident in immunohistochemical stains as a "light up" of phospho-p70^{S6K} staining in epithelial cells lining the lower 20–25% of the villi. An increase in p70^{S6K} abundance and activity occurred in the face of a significantly decreased mucosal mass, as evidenced by histological examination (Table 2) as well as by a reduced circulating level of citrulline, an amino acid that is synthesized exclusively in the intestine and serves as a marker of intestinal mass (Table 4) (46).

mTOR has been shown to regulate dietary effects on liver and muscle protein synthesis (1, 24, 24). In the intestine, increased activation of mTOR has been observed in colon cancer (16, 23). We believe that this is the first study to describe in vivo activation of this pathway in the gut during an infectious disease. In distinction to oncogenesis, the activation of this pathway in the infected intestine appears to be transient and tightly regulated, with activation for at least 5 days and a complete return to baseline by *day 11* after infection. Although we have not investigated the mechanism(s) by which rotavirus activates mTOR signaling via p70^{S6K}, there are three possiblities consistent with the published literature. First, rotavirus infection evokes a mobilization of intracellular calcium (36), a stimulator of intracellular p70^{S6K} activation. A calcium increase during rotavirus infection is known to contribute to enterocyte chloride secretion via elaboration of nonstructural protein 4. An example is angiotensin II activation of p70^{S6K} via the calcium-dependent tyrosine kinase PYK-2 in rat liver epithelial cells (18). A second possibility is that intracellular rotavirus particles produce a "stress signal" similar to ultraviolet irradiation, which activates p70^{S6K} along with JNK and ERK1 (60). Similar stress signaling has been reported with NO donors that modulate cell motility (5). Finally, when infected villus tip cells are sloughed, the migration process itself could

Table 4. *Plasma amino acid composition of fully fed, noninfected piglets and rotavirus-infected piglets*

Amino Acid	Treatment		SE	*P* Value
	Noninfected	Infected		
Aspartic acid	41.6	48.6	11.7	0.68
Glutamic acid	267.3	279.5	45.5	0.85
Asparagine	50.1	119.2	17.3	0.03
Serine	129.8*	190.5*	11.2	<0.01*
Glutamine	207.3*	429.5*	20.8	<0.01*
Histidine	52.1	83.6	10.0	0.06
Glycine	571.3	819.8	90.3	0.09
Threonine	197.7	255.3	20.5	0.09
Citrulline	129.4*	70.9*	10.1	<0.01*
Arginine	144.7	157.8	28.5	0.75
β-Alanine	42.7	24.4	6.4	0.09
Taurine	242.3	196.3	19.9	0.15
Alanine	291.8*	420.7*	34.7	0.03*
Tyrosine	150.41	133.7	23.2	0.62
Tryptophan	24.2*	31.1*	1.8	0.03*
Methionine	58.7	77.8	7.8	0.13
Valine	267.2	344.9	3.3	0.13
Phenylalanine	69.6*	109.9*	8.6	0.01*
Isoleucine	134.2	147.6	15.3	0.55
Leucine	144.5	206.3	22.9	0.10
Ornithine	126.7	87.7	17.1	0.15
Lysine	128.4	204.1	35.8	0.18
Total	3,472.1*	4,438.9*	281.1	0.05*

$n = 4$ piglets/treatment. *Amino acid levels that differed significantly.

trigger p70^{S6K} activation. This has been shown during cell spreading across the mammalian lectin galectin-8 (30), and p70^{S6K} has been shown to colocalize at the edge of migrating cells with phosphatidylinositol 3-kinase, actin, Akt1, and activated mTOR (6). It should be noted that, regardless of the mechanism, the reparative response to infection had a dominant effect compared with the level of feeding. In fact, rotaviral activation of p70^{S6K} appeared equal in malnourished compared with well-nourished piglets. However, activation by infection is probably not maximal. In unpublished studies, we were able to show in intestinal explants that p70^{S6K} from infected pigs can be activated even further by arginine or high-dose amino acids.

One interesting observation is that some viruses, such as adenovirus and rotavirus, are capable of producing proteins that mimic components of the mTOR signaling pathway and "hijack" the translational machinery (37, 56). However, rotavirus' main site of infection is the villus tip cells (10, 29), whereas we found that mTOR is activated primarily in the crypt. Furthermore, viral shedding was still present at *day 11*, even though p70^{S6K} was not phosphorylated. This finding rules against viral hijacking of the translational apparatus as the major etiology activation of mTOR that was seen at *days 3* and *5* postinoculation, because the virus was still being excreted at a time point (*day 11*) when intestinal p70^{S6K} was not phosphorylated. It should also be noted that the latex agglutination assay we used is likely to underestimate the amount of viral excretion.

Activation of this pathway appears predominant in the crypt region of the regenerating intestine. The crypt is the site of epithelial progenitor cell mitosis, a necessary event in villus cell regeneration (Fig. 3) (9). High-power microscopy of this site revealed a cytoplasmic distribution of p70^{S6K}. Activation by phosphorylation in the autoinhibitory loop (Thr^{421}/Ser^{424}) was seen in the nucleus of cells on shortened villi. We (45) have previously found nuclear phosphorylation in arginine-treated intestinal cells in culture. Although only recently published, nucleocytoplasmic shuttling has been observed for the β-isoform of p70^{S6K}(one of two S6K isoforms) after phosphorylation by PKC (55). Strong evidence for similar shuttling of mTOR has been presented, with evidence that directed mutation of the nuclear import sequence impaired activation of p70^{S6K}, whereas the structure of mTOR was not changed (3). The direct mediator of p70^{S6K} activation might be S6K-1-associated REF-like target, a nuclear protein that binds p70^{S6K}, is sensitive to rapamycin, impacts cell size, and is a member of the REF family involved in mRNA export (20, 47).

Our findings are not consistent with rotavirus-activated intestinal mTOR signaling resulting from an increase in circulating amino acid levels. We observed a marginal (29%, $P = 0.05$) increase in total amino acids that was not associated with any significant change in the two major amino acids that activate mTOR/p70^{S6K} in intestinal cells: branched-chain amino acids and L-arginine (4).

Viral Enteritis Increases Serum Glutamine and Gluconeogenic Amino Acid Levels

The small intestine is a major site for the catabolism of glutamine and the exclusive organ for its conversion into citrulline in the piglet (58). Thus, in rotavirus-infected piglets, a marked increase in the plasma glutamine level and a concomitant decrease in the citrulline level indicates reduced intestinal utilization of glutamine due to a compromised number of villus cells. In these piglets, an increase in plasma levels of all three major gluconeogenic amino acids (serine, alanine, and glutamine) suggests an increase in their release from skeletal muscle to synthesize glucose so as to meet the increased need for glucose by cells of the immune system, including lymphocytes and macrophages (15). Finally, an increase in plasma concentrations of both aromatic amino acids (tryptophan and phenylalanine), whose catabolism requires the same unique biopterin cofactor (53), suggests a relative deficiency of tetrahydrobiopterin for their utilization, likely due to an increase in its utilization for NO synthesis.

Relative Effects on p70^{S6K} Activity in the Muscle and Intestine

To determine if there was differential regulation of the mTOR pathway in the muscle and intestine during the catabolic state induced by rotavirus infection, we performed Western blot analysis using antibodies to total and phosphorylated ribosomal protein S6 (Fig. 5). We showed a dramatic effect of the infection in upregulating intestinal ribosomal protein S6 phosphorylation while downregulating skeletal muscle ribosomal protein S6 phosphorylation. A steady decrease in the muscle ribosomal protein S6 level (in all piglets, whether uninfected and infected) was seen beginning at *day 5* (corresponding to *day 10* of life), which may correspond to a decline in the very rapid protein synthesis rate seen in the first week of life (14). The observed heavy phosphorylation of muscle ribosomal protein S6 was severely inhibited during rotavirus infection (Fig. 5). We hypothesize that rotavirus infection markedly inhibits this process.

Both acute and chronic bacterial septicemia inhibit muscle protein synthesis and enhance muscle protein breakdown, concomitant with increased intestinal and liver protein synthesis (11). Furthermore, endotoxemia markedly alters mTOR pathway signaling and translation initiation in pigs (25) and rats (26). During viral enteritis, hormonal or other signals from the gut to muscle have not been investigated but could include cytokines such as IL-6, IL-1β, TNF-α, IL-12, IL-10, and IFN-γ (2, 21); reactive oxygen species; glucocorticoid hormones [which are among the best-established inhibitors of mTOR (50, 51)]; and the virus itself (8, 12). Among these, the best-recognized inhibitors of protein synthesis and mTOR in inflammatory diarrheas are glucocorticoid hormones (32, 48, 49, 52), which have been shown to inhibit the translational pathway below the level of Akt (most likely at mTOR itself) (31, 33).

In summary, our investigation demonstrated that infectious diarrhea produced an increase in intestinal protein synthesis early after viral inoculation. The increased protein synthesis appears to have preceded intestinal p70^{S6K} activation by 1–2 days. We suggest that p70^{S6K} is not a sensitive marker of level of nutrient intake (because it is not affected by formula restriction) but represents a part of the proliferative response to rotavirus enteritis. We suggest that the mTOR/p70^{S6K} pathway is markedly activated in viral enteritis, as it is in other conditions reflecting increased mitotic activity, e.g., oncogenesis. In a recent microarray study (35), gene expression profiling of the

intestinal epithelial cells along the crypt-villus axis was performed. Genes regulating ribosomal biogenesis and RNA processing were upregulated in the crypt and downregulated at the villus tip. The activation of mTOR signaling to p70^{S6K} is not generalized in the infected host, as evidenced by muscle p70^{S6K} inactivation at the same time that jejunal p70^{S6K} is activated. Our observations lead to the testable hypothesis that mTOR signaling is mechanistically important to coordinate the reciprocal regulation of muscle and intestinal protein synthesis during diarrheal disease. Clinically, the findings may be relevant to the nutritional therapy of diarrheal disease. Specifically, during acute viral diarrhea, supplementation with high levels of one or more amino acids could facilitate bowel repair and/or mitigate muscle wasting.

REFERENCES

1. **Anthony TG, Reiter AK, Anthony JC, Kimball SR, Jefferson LS.** Deficiency of dietary EAA preferentially inhibits mRNA translation of ribosomal proteins in liver of meal-fed rats. *Am J Physiol Endocrinol Metab* 281: E430–E439, 2001.
2. **Azevedo MS, Yuan L, Pouly S, Gonzales AM, Jeong KI, Nguyen TV, Saif LJ.** Cytokine responses in gnotobiotic pigs after infection with virulent or attenuated human rotavirus. *J Virol* 80: 372–382, 2006.
3. **Bachmann RA, Kim JH, Wu AL, Park IH, Chen J.** A nuclear transport signal in mammalian target of rapamycin is critical for its cytoplasmic signaling to S6 kinase 1. *J Biol Chem* 281: 7357–7363, 2006.
4. **Ban H, Shigemitsu K, Yamatsuji T, Haisa M, Nakajo T, Takaoka M, Nobuhisa T, Gunduz M, Tanaka N, Naomoto Y.** Arginine and leucine regulate p70 S6 kinase and 4E-BP1 in intestinal epithelial cells. *Int J Mol Med* 13: 537–543, 2004.
5. **Berven LA, Frew IJ, Crouch MF.** Nitric oxide donors selectively potentiate thrombin-stimulated p70^{S6k} activity and morphological changes in Swiss 3T3 cells. *Biochem Biophys Res Commun* 266: 352–360, 1999.
6. **Berven LA, Willard FS, Crouch MF.** Role of the p70^{S6K} pathway in regulating the actin cytoskeleton and cell migration. *Exp Cell Res* 296: 183–195, 2004.
7. **Blikslager AT, Roberts MC, Young KM, Rhoads JM, Argenzio RA.** Genistein augments prostaglandin-induced recovery of barrier function in ischemia-injured porcine ileum. *Am J Physiol Gastrointest Liver Physiol* 278: G207–G216, 2000.
8. **Blutt SE, Kirkwood CD, Parreno V, Warfield KL, Ciarlet M, Estes MK, Bok K, Bishop RF, Conner ME.** Rotavirus antigenaemia and viraemia: a common event? *Lancet* 362: 1445–1449, 2003.
9. **Boshuizen JA, Reimerink JH, Korteland-van Male AM, van Ham VJ, Bouma J, Gerwig GJ, Koopmans MP, Buller HA, Dekker J, Einerhand AW.** Homeostasis and function of goblet cells during rotavirus infection in mice. *Virology* 337: 210–221, 2005.
10. **Boshuizen JA, Rossen JW, Sitaram CK, Kimenai FF, Simons-Oosterhuis Y, Laffeber C, Buller HA, Einerhand AW.** Rotavirus enterotoxin NSP4 binds to the extracellular matrix proteins laminin-beta3 and fibronectin. *J Virol* 78: 10045–10053, 2004.
11. **Breuille D, Arnal M, Rambourdin F, Bayle G, Levieux D, Obled C.** Sustained modifications of protein metabolism in various tissues in a rat model of long-lasting sepsis. *Clin Sci (Lond)* 94: 413–423, 1998.
12. **Crawford SE, Patel DG, Cheng E, Berkova Z, Hyser JM, Ciarlet M, Finegold MJ, Conner ME, Estes MK.** Rotavirus viremia and extraintestinal viral infection in the neonatal rat model. *J Virol* 80: 4820–4832, 2006.
13. **Davidson GP, Gall DG, Petric M, Butler DG, Hamilton JR.** Human rotavirus enteritis induced in conventional piglets. Intestinal structure and transport. *J Clin Invest* 60: 1402–1409, 1977.
14. **Davis TA, Burrin DG, Fiorotto ML, Nguyen HV.** Protein synthesis in skeletal muscle and jejunum is more responsive to feeding in 7-than in 26-day-old pigs. *Am J Physiol Endocrinol Metab* 270: E802–E809, 1996.
15. **Dugan ME, Knabe DA, Wu G.** Glutamine and glucose metabolism in intraepithelial lymphocytes from pre- and post-weaning pigs. *Comp Biochem Physiol B Biochem Mol Biol* 109: 675–681, 1994.
16. **Fukuda R, Hirota K, Fan F, Jung YD, Ellis LM, Semenza GL.** Insulin-like growth factor 1 induces hypoxia-inducible factor 1-mediated vascular endothelial growth factor expression, which is dependent on MAP kinase and phosphatidylinositol 3-kinase signaling in colon cancer cells. *J Biol Chem* 277: 38205–38211, 2002.
17. **Gookin JL, Rhoads JM, Argenzio RA.** Inducible nitric oxide synthase mediates early epithelial repair of porcine ileum. *Am J Physiol Gastrointest Liver Physiol* 283: G157–G168, 2002.
18. **Graves LM, He Y, Lambert J, Hunter D, Li X, Earp HS.** An intracellular calcium signal activates p70 but not p90 ribosomal S6 kinase in liver epithelial cells. *J Biol Chem* 272: 1920–1928, 1997.
19. **Greene HL, McCabe DR, Merenstein GB.** Protracted diarrhea and malnutrition in infancy: changes in intestinal morphology and disaccharidase activities during treatment with total intravenous nutrition or oral elemental diets. *J Pediatr* 87: 695–704, 1975.
20. **Hunter RJ, Patel VB, Miell JP, Wong HJ, Marway JS, Richardson PJ, Preedy VR.** Diarrhea reduces the rates of cardiac protein synthesis in myofibrillar protein fractions in rats in vivo. *J Nutr* 131: 1513–1519, 2001.
21. **Jiang B, Snipes-Magaldi L, Dennehy P, Keyserling H, Holman RC, Bresee J, Gentsch J, Glass RI.** Cytokines as mediators for or effectors against rotavirus disease in children. *Clin Diagn Lab Immunol* 10: 995–1001, 2003.
22. **Kerzner B, Kelly MH, Gall DG, Butler DG, Hamilton JR.** Transmissible gastroenteritis: sodium transport and the intestinal epithelium during the course of viral enteritis. *Gastroenterology* 72: 457–461, 1977.
23. **Khaleghpour K, Li Y, Banville D, Yu Z, Shen SH.** Involvement of the PI 3-kinase signaling pathway in progression of colon adenocarcinoma. *Carcinogenesis* 25: 241–248, 2004.
24. **Kimball SR, Jefferson LS, Nguyen HV, Suryawan A, Bush JA, Davis TA.** Feeding stimulates protein synthesis in muscle and liver of neonatal pigs through an mTOR-dependent process. *Am J Physiol Endocrinol Metab* 279: E1080–E1087, 2000.
25. **Kimball SR, Orellana RA, O'Connor PM, Suryawan A, Bush JA, Nguyen HV, Thivierge MC, Jefferson LS, Davis TA.** Endotoxin induces differential regulation of mTOR-dependent signaling in skeletal muscle and liver of neonatal pigs. *Am J Physiol Endocrinol Metab* 285: E637–E644, 2003.
26. **Lang CH, Frost RA.** Endotoxin disrupts the leucine-signaling pathway involving phosphorylation of mTOR, 4E-BP1, and S6K1 in skeletal muscle. *J Cell Physiol* 203: 144–155, 2005.
27. **Lecce JG, Balsbaugh RK, Clare DA, King MW.** Rotavirus and hemolytic enteropathogenic *Escherichia coli* in weanling diarrhea of pigs. *J Clin Microbiol* 16: 715–723, 1982.
28. **Lecce JG, King MW.** Role of rotavirus (reo-like) in weanling diarrhea of pigs. *J Clin Microbiol* 8: 454–458, 1978.
29. **Lecce JG, King MW, Dorsey WE.** Rearing regimen producing piglet diarrhea (rotavirus) and its relevance to acute infantile diarrhea. *Science* 199: 776–778, 1978.
30. **Levy Y, Ronen D, Bershadsky AD, Zick Y.** Sustained induction of ERK, protein kinase B, and p70 S6 kinase regulates cell spreading and formation of F-actin microspikes upon ligation of integrins by galectin-8, a mammalian lectin. *J Biol Chem* 278: 14533–14542, 2003.
31. **Liu Z, Jahn LA, Long W, Fryburg DA, Wei L, Barrett EJ.** Branched chain amino acids activate messenger ribonucleic acid translation regulatory proteins in human skeletal muscle, and glucocorticoids blunt this action. *J Clin Endocrinol Metab* 86: 2136–2143, 2001.
32. **Liu Z, Li G, Kimball SR, Jahn LA, Barrett EJ.** Glucocorticoids modulate amino acid-induced translation initiation in human skeletal muscle. *Am J Physiol Endocrinol Metab* 287: E275–E281, 2004.
33. **Liu Z, Li G, Kimball SR, Jahn LA, Barrett EJ.** Glucocorticoids modulate amino acid-induced translation initiation in human skeletal muscle. *Am J Physiol Endocrinol Metab* 287: E275–E281, 2004.
34. **Lo CW, Walker WA.** Chronic protracted diarrhea of infancy: a nutritional disease. *Pediatrics* 72: 786–800, 1983.
35. **Mariadason JM, Nicholas C, L'Italien KE, Zhuang M, Smartt HJ, Heerdt BG, Yang W, Corner GA, Wilson AJ, Klampfer L, Arango D, Augenlicht LH.** Gene expression profiling of intestinal epithelial cell maturation along the crypt-villus axis. *Gastroenterology* 128: 1081–1088, 2005.
36. **Morris AP, Estes MK.** Microbes and microbial toxins: paradigms for microbial-mucosal interactions. VIII. Pathological consequences of rotavirus infection and its enterotoxin. *Am J Physiol Gastrointest Liver Physiol* 281: G303–G310, 2001.
37. **O'Shea C, Klupsch K, Choi S, Bagus B, Soria C, Shen J, McCormick F, Stokoe D.** Adenoviral proteins mimic nutrient/growth signals to activate the mTOR pathway for viral replication. *EMBO J* 24: 1211–1221, 2005.

38. **Oliver WT, Mathews SA, Phillips O, Jones EE, Odle J, Harrell RJ.** Efficacy of partially hydrolyzed corn syrup solids as a replacement for lactose in manufactured liquid diets for neonatal pigs. *J Anim Sci* 80: 143–153, 2002.
39. **Peterson RT, Desai BN, Hardwick JS, Schreiber SL.** Protein phosphatase 2A interacts with the 70-kDa S6 kinase and is activated by inhibition of FKBP12-rapamycinassociated protein. *Proc Natl Acad Sci USA* 96: 4438–4442, 1999.
40. **Rao JN, Guo X, Liu L, Zou T, Murthy KS, Yuan JX, Wang JY.** Polyamines regulate Rho-kinase and myosin phosphorylation during intestinal epithelial restitution. *Am J Physiol Cell Physiol* 284: C848–C859, 2003.
41. **Rao JN, Li J, Li L, Bass BL, Wang JY.** Differentiated intestinal epithelial cells exhibit increased migration through polyamines and myosin II. *Am J Physiol Gastrointest Liver Physiol* 277: G1149–G1158, 1999.
42. **Rhoads JM, Chen W, Gookin J, Wu GY, Fu Q, Blikslager AT, Rippe RA, Argenzio RA, Cance WG, Weaver EM, Romer LH.** Arginine stimulates intestinal cell migration through a focal adhesion kinase dependent mechanism. *Gut* 53: 514–522, 2004.
43. **Rhoads JM, Gomez GG, Chen W, Goforth R, Argenzio RA, Neylan MJ.** Can a super oral rehydration solution stimulate intestinal repair in acute viral enteritis? *J Diarrhoeal Dis Res* 14: 175–181, 1996.
44. **Rhoads JM, Keku EO, Quinn J, Woosely J, Lecce JG.** L-Glutamine stimulates jejunal sodium and chloride absorption in pig rotavirus enteritis. *Gastroenterology* 100: 683–691, 1991.
45. **Rhoads JM, Niu X, Odle J, Graves LM.** Role of mTOR signaling in intestinal cell migration. *Am J Physiol Gastrointest Liver Physiol* 291: G510–G517, 2006.
46. **Rhoads JM, Plunkett E, Galanko J, Lichtman S, Taylor L, Maynor A, Weiner T, Freeman K, Guarisco JL, Wu GY.** Serum citrulline levels correlate with enteral tolerance and bowel length in infants with short bowel syndrome. *J Pediatr* 146: 542–547, 2005.
47. **Richardson CJ, Broenstrup M, Fingar DC, Julich K, Ballif BA, Gygi S, Blenis J.** SKAR is a specific target of S6 kinase 1 in cell growth control. *Curr Biol* 14: 1540–1549, 2004.
48. **Shah OJ, Anthony JC, Kimball SR, Jefferson LS.** 4E-BP1 and S6K1: translational integration sites for nutritional and hormonal information in muscle. *Am J Physiol Endocrinol Metab* 279: E715–E729, 2000.
49. **Shah OJ, Anthony JC, Kimball SR, Jefferson LS.** Glucocorticoids oppose translational control by leucine in skeletal muscle. *Am J Physiol Endocrinol Metab* 279: E1185–E1190, 2000.
50. **Shah OJ, Anthony JC, Kimball SR, Jefferson LS.** Glucocorticoids oppose translational control by leucine in skeletal muscle. *Am J Physiol Endocrinol Metab* 279: E1185–E1190, 2000.
51. **Shah OJ, Kimball SR, Jefferson LS.** Among translational effectors, p70S6k is uniquely sensitive to inhibition by glucocorticoids. *Biochem J* 347: 389–397, 2000.
52. **Shah OJ, Kimball SR, Jefferson LS.** Among translational effectors, p70S6k is uniquely sensitive to inhibition by glucocorticoids. *Biochem J* 347: 389–397, 2000.
53. **Shi W, Meininger CJ, Haynes TE, Hatakeyama K, Wu G.** Regulation of tetrahydrobiopterin synthesis and bioavailability in endothelial cells. *Cell Biochem Biophys* 41: 415–434, 2004.
54. **Talarico TL, Dobrogosz WJ.** Chemical characterization of an antimicrobial substance produced by *Lactobacillus reuteri*. *Antimicrob Agents Chemother* 33: 674–679, 1989.
55. **Valovka T, Verdier F, Cramer R, Zhyvoloup A, Fenton T, Rebholz H, Wang ML, Gzhegotsky M, Lutsyk A, Matsuka G, Filonenko V, Wang L, Proud CG, Parker PJ, Gout IT.** Protein kinase C phosphorylates ribosomal protein S6 kinase betaII and regulates its subcellular localization. *Mol Cell Biol* 23: 852–863, 2003.
56. **Varani G, Allain FH.** How a rotavirus hijacks the human protein synthesis machinery. *Nat Struct Biol* 9: 158–160, 2002.
57. **Wang JY, Wang J, Golovina VA, Li L, Platoshyn O, Yuan JX.** Role of K^+ channel expression in polyamine-dependent intestinal epithelial cell migration. *Am J Physiol Cell Physiol* 278: C303–C314, 2000.
58. **Wu G.** Intestinal mucosal amino acid catabolism. *J Nutr* 128: 1249–1252, 1998.
59. **Wu G, Knabe DA.** Free and protein-bound amino acids in sow's colostrum and milk. *J Nutr* 124: 415–424, 1994.
60. **Zhang Y, Dong Z, Nomura M, Zhong S, Chen N, Bode AM, Dong Z.** Signal transduction pathways involved in phosphorylation and activation of p70S6K following exposure to UVA irradiation. *J Biol Chem* 276: 20913–20923, 2001.
61. **Zijlstra RT, Donovan SM, Odle J, Gelberg HB, Petschow BW, Gaskins HR.** Protein-energy malnutrition delays small-intestinal recovery in neonatal pigs infected with rotavirus. *J Nutr* 127: 1118–1127, 1997.
62. **Zijlstra RT, McCracken BA, Odle J, Donovan SM, Gelberg HB, Petschow BW, Zuckermann FA, Gaskins HR.** Malnutrition modifies pig small intestinal inflammatory responses to rotavirus. *J Nutr* 129: 838–843, 1999.